where $V_0e^{-i\mathbf{q}\cdot\mathbf{r}}$ is the applied potential and $V_{\text{int}}(\mathbf{r})e^{-i\mathbf{q}\cdot\mathbf{r}}$ is the screening potential. Proceeding as before, we get

$$\langle l|\rho_1|l'\rangle=F_{l'l}\langle l|V|l'\rangle \approx F_{l'l}e^{-i\mathbf{q}\cdot\mathbf{R}}[-i\mathbf{q}\cdot\mathbf{X}_{ll'}V_0+\langle l|V_{\text{int}}|l'\rangle], \quad \text{(B2)}$$

and

$$n(\mathbf{r})=\sum_{l'l}\psi_{l'}^*(\mathbf{r})\psi_l(\mathbf{r})\langle l|\rho_1|l'\rangle = e^{-i\mathbf{q}\cdot\mathbf{r}}\sum_{l'l}\psi_{l'}^*(\mathbf{r})\psi_l(\mathbf{r}) \times e^{-i\mathbf{q}\cdot(\mathbf{r}-\mathbf{R})}F_{l'l}[-i\mathbf{q}\cdot\mathbf{X}_{ll'}V_0+\langle l|V_{\text{int}}|l'\rangle]. \quad \text{(B3)}$$

Next, we average $n(\mathbf{r})$ to obtain

$$\bar{n}\approx e^{-i\mathbf{q}\cdot\mathbf{R}}i\Delta^{-1}\sum_{l'l}F_{l'l}\mathbf{q}\cdot\mathbf{X}_{ll'} \times[-i\mathbf{q}\cdot\mathbf{X}_{ll'}V_0+\langle l|V_{\text{int}}|l'\rangle], \quad \text{(B4)}$$

where the bar here denotes an average taken over the region occupied by the atom, whose location is given by the macroscopic position variable $\mathbf{R}$. Finally, relating $\bar{n}$ to $\bar{P}$ and V_0 to $\bar{E}_0$ gives

$$p=\bar{P}\Delta=(e^2/m^2)\sum_{l'l}F_{l'l}|P_{l'l}^{\mu}|^2\omega_{l'l}^{-2}\bar{E}_0 -e^2\sum_{l'l}F_{l'l}X_{l'l}^{\mu}e^{-i\mathbf{q}\cdot\mathbf{R}}\langle l|-e^{-1}V_{\text{int}}|l'\rangle, \quad \text{(B5)}$$

where p is the dipole moment of the atom. Use was again made of Eq. (67).

By definition, the ratio of the dipole moment to the macroscopic applied field is just the polarizability. The first term in Eq. (B5) arises directly from the applied field, showing that

$$\alpha=(e^2/m^2)\textstyle\sum_{l'l}F_{l'l}|P_{l'l}^{\mu}|^2\omega_{l'l}^{-2}. \quad \text{(B6)}$$

The second term arises from the field caused by the self-consistent response of the electrons, showing it to be a self-polarization effect. In our linear treatment, the matrix element of V_{int} must be proportional to $\bar{E}_0$ giving the desired result,

$$\alpha_{\text{sp}}\bar{E}_0=e^2\textstyle\sum_{l'l}F_{l'l}X_{l'l}^{\mu}e^{-i\mathbf{q}\cdot\mathbf{R}}\langle l|-e^{-1}V_{\text{int}}|l'\rangle. \quad \text{(B7)}$$

PHYSICAL REVIEW VOLUME 129, NUMBER 1 1 JANUARY 1963

Optical Properties of the Silver and Cuprous Halides

MANUEL CARDONA
RCA Laboratories, Princeton, New Jersey
(Received 13 August 1962)

The exciton spectrum of AgI, CuI, CuBr, and CuCl is discussed and various peaks attributed to several coexisting crystal modifications. The shift of the peaks with alloy concentration in the pseudobinary systems formed with these compounds is reported and interpreted. The absorption and reflection spectra of these materials and their alloys for energies between the energy gap and 10 eV is reported and the structure attributed to transitions between regions of the valence band lying below the highest maximum and parts of the conduction band higher than the lowest minimum. These spectra are compared with the corresponding spectra of other zincblende- and wurtzite-like materials.

I. INTRODUCTION

THE silver and cuprous halides are members of a family of semiconductors which has received much attention: the semiconductors with four valence electrons per atom. Among these semiconductors are the elementary semiconductors of the fourth group of the periodic table (diamond, Si, Ge, and gray tin) which crystallize in the diamond lattice. The next members of the family are the so-called III-V semiconductors whose unit cell has one atom of the third group and one of the fifth group. Most of these semiconductors crystallize in the zincblende lattice at normal conditions, but a few (among those of high band gap and high melting point) crystallize in the wurtzite (AlN, GaN, and InN) and other more complicated structures (BAs, BN). The next members in the direction of increasing polarity are the II-VI compounds which crystallize ordinarily in the zincblende or the wurtzite structures. Some of these compounds may exist at room temperature in both forms, one of them metastable.

The intrinsic reflection and transmission spectra of all these semiconductors with zincblende structure exhibit a striking systematic similarity.[1-4] The lowest-energy direct absorption edge, due to transitions at $k=0$, shows a splitting which can be correlated with the spin-orbit splitting of the constituent atoms. The next absorption edge has been attributed to direct transitions at a point in the [111] direction of k space: This edge has a splitting which is approximately two-

[1] M. Cardona, Suppl. J. Appl. Phys. **32**, 2151 (1961).
[2] M. Cardona and D. L. Greenaway, Phys. Rev. **125**, 1291 (1962).
[3] H. Ehrenreich, H. R. Phillipp, and J. C. Phillips, Phys. Rev. Letters **8**, 59 (1962).
[4] M. Cardona and G. Harbeke, Phys. Rev. Letters **8**, 90 (1962).

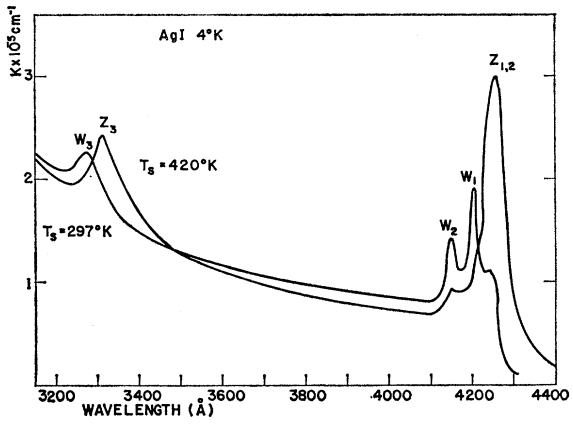

FIG. 1. Exciton spectrum of AgI at 4°K.

thirds of the splitting of the $k=0$ edge, in agreement with theoretical predictions for the spin-orbit splitting of the valence band at a point in the [111] direction remote from $k=0$. Sometimes (Si, C, GaP, ZnS) the [111] edge is hidden under a stronger absorption due to transitions at $k=0$. Next towards increasing photon energies one finds a maximum in the absorption, due to a maximum in the combined density of states for the transitions near the (1,0,0) point of the Brillouin zone. After this peak, another edge appears which has been attributed to transitions in the [111] direction between the highest valence band and the second lowest conduction band: This edge has the same splitting as the lower [111] edge. A break in the systematics of the zincblende semiconductors for the copper halides has been pointed out[5]: The first absorption edge occurs at much lower energy than expected by extrapolating the corresponding edge of the isoelectronic II-VI compounds. It has been suggested that this anomaly is caused by the weakly bound 3d electrons of the copper.

The purpose of his paper is to study the absorption and reflection spectra of the cuprous and silver halides with zincblende structure from the lowest edge to 10 eV, to interpret these spectra in terms of the band structure of the compounds, and to discuss the systematics of the band structure of the zincblende-type semiconductors.

II. CRYSTAL MODIFICATIONS OF THE SILVER AND CUPROUS HALIDES

Silver fluoride, chloride, and bromide crystallize only in the rock salt structure. Their optical properties and band structures are similar to the alkali halides[6] and will not be treated in this paper. Silver iodide has three known modifications at normal pressure.[7] Up to 408°K the stable modification has the zincblende lattice (γ-AgI). From 408 to 419°K the stable modification has the wurtzite lattice (β-AgI) and above 419°K the material crystallizes in a complicated structure with a body-centered cubic unit cell with a statistical distribution of Ag atoms in several possible positions. This crystal structure is normally referred to as the AgI lattice (α-AgI). A similar situation occurs in CuBr where the γ phase is stable up to 664°K, the β phase between 664 and 743°K and the α phase above 743°K.[8] CuI has the same phases[9] (γ between about room temperature and 643°K, β between 643 and 703°K, and α above 703°K) plus a hexagonal layer structure[10] at room temperature similar to the wurtzite and zincblende lattices but with a different layer sequence. CuCl has zincblende structure up to 680°K and wurtzite structure from 680°K up to the melting point.[11]

A zincblende variety of CuF has been reported in the literature[12] but the existence of any variety of CuF under normal conditions has been questioned by a number of authors[13]; CuF decomposes into CuF_2 and copper. The x-ray patterns attributed to CuF seem to be due to the presence of Cu_2O. Several attempts we made to prepare CuF were unsuccessful.

III. MEASUREMENTS

Samples of CuCl, CuBr, CuI, AgI and their alloys were prepared by evaporating the material in powder from Fisher Scientific Company, New York, N. Y. onto a heated substrate. Fused quartz was used as a substrate for measurements in the visible and near ultraviolet, calcium fluoride for measurements in the vacuum ultraviolet.

Optical measurements in the visible and near ultraviolet were made with a Cary 14M spectrophotometer. Measurements in the vacuum uv were performed with a Jarrell-Ash vacuum uv spectrometer, the light source being a Tanaka hydrogen arc and the detector, a sodium salicylate coated photomultiplier. A special attachment was built which measured the reflectivity of the sample in vacuum by moving the photomultiplier from the incident beam to the reflected beam.

The thickness of the evaporated films was determined by the Tolansky method.

IV. EXCITON SPECTRUM

A. Pure Compounds

The existence of exciton peaks at the absorption edge of AgI, CuI, CuBr, and CuCl has been reported by

[5] F. Herman and D. S. McClure, Bull. Am. Phys. Soc. **5**, 48 (1960).
[6] Y. Okamoto, Nachr. Akad. Wiss. Gottingen, Math. Physik. Kl. **14**, 275 (1956).
[7] R. Bloch and H. Möller, Z. Physik. Chem. **A152**, 2-5 (1931).
[8] J. Krug and L. Sieg, Z. Naturforsch. **7a**, 369 (1952).
[9] S. Miyake, S. Hoshino, and T. Takenaka, J. Phys. Soc. Japan **7**, 19 (1952).
[10] R. N. Kurdyumova and R. V. Baranova, Soviet Phys.—Cryst. **6**, 318 (1961).
[11] M. R. Lorenz and J. S. Prener, Acta Cryst. **9**, 538 (1956).
[12] F. Ebert and H. Woitinek, Z. Anorg. Allg. Chem. **210**, 263 (1933).
[13] J. M. Crabtree, J. Inorg. Nuclear Chem. **1**, 213 (1955).

several authors.[14] In this section we shall report some new lines in these spectra and interpret them in terms of the presence of several crystal modifications in the samples. Figure 1 shows the exciton absorption spectrum of two AgI evaporated layers at liquid-helium temperatures. One of them was evaporated onto a substrate at $T_s=420°K$ and the other at $T_s=297°K$. The samples evaporated at $T_s=420°K$ condense as a bright yellow layer of α-AgI. After cooling to room temperature, they transform mostly into γ-AgI (zincblende) with a small amount of β-AgI (wurtzite) as evidenced by a Debye-Scherrer picture of powder scraped from the substrate. The layers are highly oriented with the [111] axis perpendicular to the substrate. The layers evaporated at $T_s=297°K$ condense mostly as β-AgI, which is not stable at this temperature, with a small amount of γ-AgI. The rate with which the unstable β-AgI transforms into γ-AgI at room temperature must be very small, since the transformation could not be observed. It follows clearly from Fig. 1 that the exciton peaks $Z_{1,2}$ and Z_3 belong to the γ-AgI phase since they are very strong in the sample with high γ-AgI content. The W_1, W_2, and W_3 peaks belong to the β-AgI modification. This is in agreement with the results of Maier and Waidelich[15] for the $Z_{1,2}$, W_1, and W_2 peaks but disagrees with the results of Perny[16] who attributed all of these lines to the cubic phase.

This exciton spectrum can be interpreted along the same lines as the absorption edge of other materials with wurtzite and zincblende structures. The strength of the exciton spectrum suggests direct allowed transitions which, by analogy with the other zincblende and wurtzite materials, should occur at $k=0$. The top of the valence band (Γ_{15}) is triply degenerate without spin-orbit interaction in the zincblende structure. This degeneracy is reduced by spin-orbit splitting to a doubly degenerate state (Γ_8) and a singlet (Γ_6). The Γ_8 doublet gives the $Z_{1,2}$ peak whose degeneracy is lifted in strained samples.[16]

The wurtzite band structure can be approximately derived by adding a perturbing trigonal crystal field to the corresponding zincblende structure.[17] This field splits the Γ_8 doublet into two (Γ_7 and Γ_9) and displaces its middle point. The W_1 peak in Fig. 1 can be identified with the Γ_9 valence band state, W_2 with the Γ_7 state, and W_3 with the lower Γ_7 state. The interval between the Γ_7 and Γ_9 peaks (0.036 eV), giving the crystal field splitting of the $Z_{1,2}$ doublet, is close to the splitting found in other wurtzite materials (0.025 eV in CdSe,[18] 0.03 eV in ZnS[19]) The shift of the center of the doublet

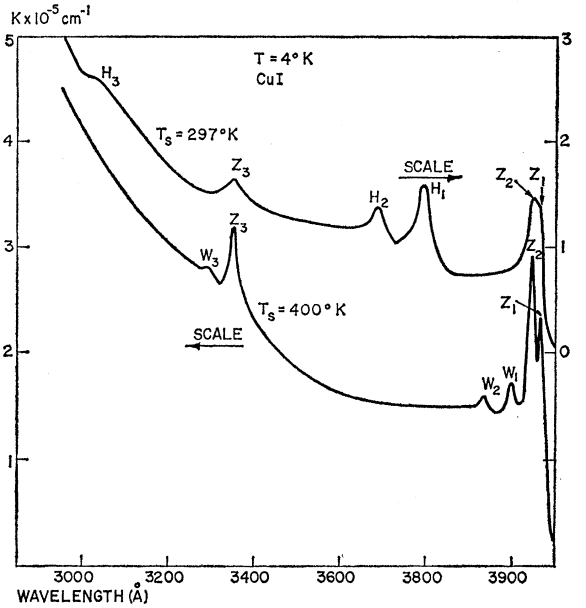

FIG. 2. Exciton spectrum of CuI at 4°K.

under the influence of the trigonal field is 0.047 and the shift of the Z_3 line is 0.03 eV, which is also close to the corresponding shift in ZnS (0.035 eV).[19]

Figure 2 shows the exciton spectrum of two CuI samples at liquid helium temperature. The sample evaporated with a substrate temperature $T_s=400°K$ shows a structure very similar to the AgI samples. The $Z_{1,2}$ doublet is split, probably due to the strain arising from the differential contraction of the substrate and the specimen. Hence, it is logical to attribute these lines to the same mechanism as the AgI lines and to postulate the presence of a small, unstable amount of wurtzite-type CuI in the sample. This could not be confirmed by x-ray analysis since the estimated accuracy of this procedure ($\sim 5\%$) was too small and the possibility exists that the wurtzite phase transforms into γ-CuI while scraping it from the substrate. The W_1, W_2, and W_3 lines were not present in samples evaporated at 473°K. Further evidence supporting this conclusion is presented in Sec. IV B in connection with measurements on CuI-AgI alloys. The crystal field splitting of the W_1–W_2 doublet is 0.048 eV and the shift in the center of the doublet under the trigonal field 0.069 eV. The shift of the Z_3 peak is 0.064 eV.

The CuI sample evaporated at room temperature does not show the W_1, W_2, and W_3 peaks. Instead, the H_1, H_2 doublet and the H_3 peak appear. Those peaks are probably due to the presence of the hexagonal layer structure whose existence has been found at room temperature.[10,20] The trigonal crystal field that one has to apply to the zincblende lattice in order to obtain the H

[14] S. Nikitine, *Progress in Semiconductors*, edited by A. F. Gibson (John Wiley & Sons, Inc., New York, 1962), Vol. 6.
[15] G. Maier and W. Waidelich, Z. Naturforsch. **13a**, 562 (1958).
[16] G. Perny, J. Chim. Phys. **55**, 650 (1958).
[17] J. L. Birman, J. Phys. Chem. Solids **8**, 35 (1959).
[18] J. O. Dimmock and R. G. Wheeler, Suppl. J. Appl. Phys. **32**, 2271 (1961).
[19] J. A. Beun and G. J. Goldsmith, Helv. Phys. Acta. **33**, 508 (1960).
[20] R. Coelho, Massachusetts Institute of Technology, Laboratory for Insulation Research, Technical Report 143, October, 1959 (unpublished).

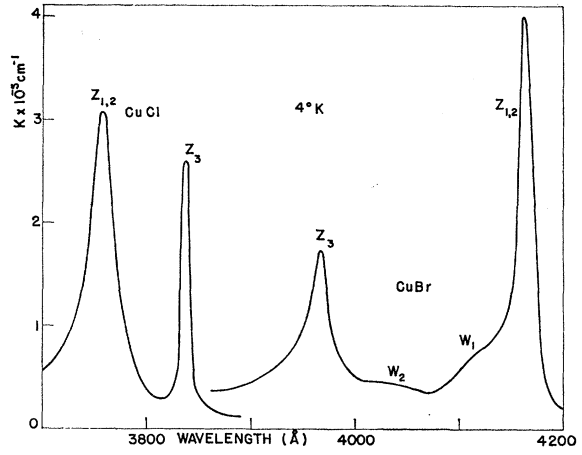

FIG. 3. Exciton spectrum of CuBr and CuCl at 4°K.

structure seems to be much larger than that to obtain the wurtzite structure if we assume that the H_1–H_2 doublet has been obtained from the $Z_{1,2}$ line and H_3 from the Z_3 line. Calling δ_1 the splitting of the doublet and δ_2 the shift of its center we have

$$\left[\frac{\delta_1(H_{1,2})}{\delta_1(W_{1,2})}\right]^2=3.9\approx\frac{\delta_2(H_{1,2})}{\delta_2(W_{1,2})}=3.7.$$

Assuming that the perturbing field is of the same form in the W as in the H structure but of different intensity, we must conclude that δ_1 arises from a first-order perturbation and δ_2 is the result of a second-order perturbation on the zincblende potential.

Figure 3 shows the exciton spectrum of CuCl and CuBr at liquid-helium temperature. Both samples were prepared with the substrate at $T_s=373$°K. The CuBr spectrum shows two strong peaks. The low-energy peak splits for samples annealed at 473°K in order to introduce strains when cooled.[20] It therefore seems reasonable to identify the $Z_{1,2}$ doublet with the Γ_8 valence band doublet of the zincblende structure and the Z_3 peaks with the spin-orbit split Γ_6 state. Two weak lines W_1 and W_2 appear at 4050 and 4120 Å. By comparing them to the W_1 and W_2 lines of CuI and AgI, we conclude that in CuBr these lines are also probably due to the presence of a small amount of wurtzite phase: The doublet splitting is 0.05 eV and its shift is 0.065 eV. These lines have already been reported by Reiss.[21]

The most salient feature of the CuCl spectrum is the fact that the strongest of the two lines is the high-energy line while in CuBr, CuI, and AgI the strongest line ($Z_{1,2}$) is the lowest energy one. Since the strongest line should be the doublet line because of the larger number of states available for transitions from the doubly degenerate valence band, we conclude that the triplet in CuCl is inverted. Further evidence supporting this conclusion will be presented in Sec. IV B in connection with measurements in CuBr–CuCl alloys. According to this conclusion, CuCl is the only known zincblende-type semiconductor with a nondegenerate highest valence band at $k=0$. The extreme sharpness of the Z_3 peak is due to this peculiarity, since electrons at the top of the valence band can only be scattered to states within the same band. The number of states to be scattered to when this band is lower in energy is much larger since, now, electrons can be scattered from it to the degenerate bands. The scattering time in the degenerate bands must also be smaller because of the larger number of states available for scattering. The larger scattering time decreases the indeterminacy broadening of the line. The $Z_{1,2}$ line in CuCl shows some evidence of a splitting in some of the samples measured. However, the splitting could not be seen as clearly as in the other materials reported, due to the large broadening of the Γ_8 state when its energy is below that of the Γ_6 state.

The one-electron spin-orbit splitting parameters of Cl, Br, and I are 0.11, 0.45, and 0.94 eV, respectively. The spin-orbit splittings in zincblende and wurtzite-type crystals are obtained by mutliplying the one-electron atomic splitting parameter by 1.5.[22] The experimental splittings are considerably smaller than the halogen splittings; therefore the valence band wave functions at $k=0$ must, in the tight-binding approximation, be formed from halogen wave functions with a large proportion of metal wave functions. The energy interval between the ground state of the Cu^+ ion ($3d^{10}$)

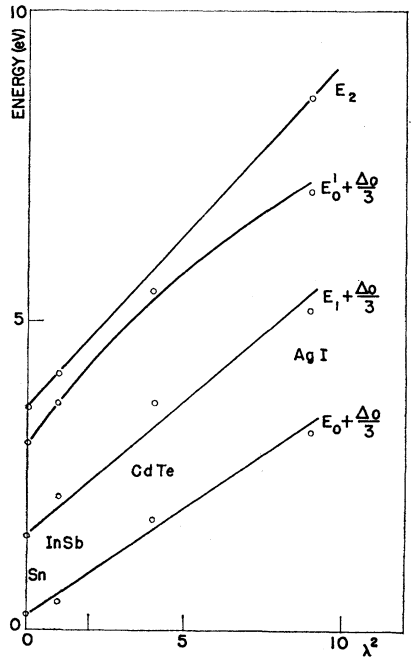

FIG. 4. Main peaks in the absorption spectrum of the AgI isoelectronic sequence (corrected for spin-orbit splitting.)

[21] R. Reiss, thesis, University of Paris, 1959 (unpublished).

[22] R. Braunstein, J. Phys. Chem. Solids 8, 280 (1959).

and the first excited state ($3d^9 4s$) is 2.75 eV.[23] This fact induced Herman and McClure[5] to postulate that the exciton peaks are due to transitions within the Cu^+ ion. The correlation between the $Z_{1,2}-Z_3$ splittings and the halogen splittings is evidence against this hypothesis, and we must admit that the valence band wave functions are formed by a strong admixture of metal and halogen wave functions. This also explains the break in the systematics of the gaps of zincblende-type semiconductors, which, according to Herman should be given by[24]

$$E_{\text{polar}}=E_{\text{nonpolar}}+A\lambda^2, \qquad (1)$$

where E_{nonpolar} is the gap of the corresponding isoelectronic semiconductor of the fourth column, A is a constant for each isoelectronic sequence and $\lambda=1$ for the III-V compounds, 2 for the II-VI compounds, and 3 for copper and silver halides. The gaps predicted for the copper halides using Eq. (1) are much larger than the energies at which the exciton peaks occur. The energy interval between the $4d^{10}$ level in Ag^+ and the first excited state ($4d^9 5s$) is 5 eV,[25] hence the contribution of the Ag wave functions to the valence band wave functions should be small: Eq. (1) holds reasonably well for the energy gap E_0 (corrected for spin-orbit splitting[2]) of the AgI isoelectronic sequence, as shown in Fig. 4.

The inverted nature of the Z triplet in CuCl seems to indicate that the copper contributes a negative term to the spin-orbit splitting of the compound, since for this material the anion splitting is small and negative. We can estimate the "fraction" of metal wave function in the valence band states by writing the spin-orbit splitting of the compound as:

$$\Delta_0=3/2[\alpha\Delta_{\text{halogen}}-(1-\alpha)\Delta_{\text{metal}}], \qquad (2)$$

where α is the proportion of halogen in the wave function or the relative amount of time spent by the valence band electrons around the halogen, Δ_{halogen} is the one-electron atomic spin-orbit splitting parameter of the halogen and Δ_{metal} the one of the d electrons of the metal (0.10 eV for Cu, 0.23 eV for Ag). From Eq. (2) we obtain $\alpha=0.25$ for CuCl, 0.36 for CuBr, 0.50 for CuI, and 0.68 for AgI. α decreases with increasing electron affinity of the halogen. This explains the almost equal energy gap found for CuCl, CuBr, and CuI[26]: While increasing the electron affinity of the halogen increases the energy gap, the increasing admixture of metal d wave function in the valence band decreases it, giving an almost constant gap. The covalency of the binding decreases with increasing α and, by extrapolation, should be very small

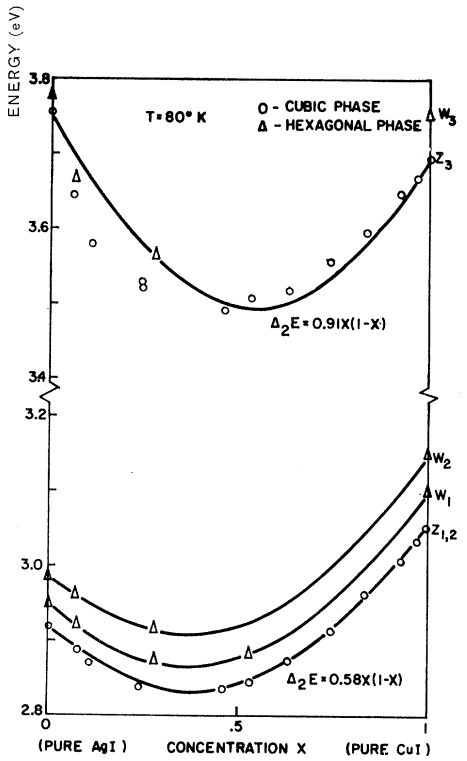

FIG. 5. Energy of the exciton peaks vs concentration in the AgI-CuI system.

in AgCl and AgBr crystallized in the zincblende structure. This explains why these compounds crystallize in the rock salt structure which corresponds to predominantly polar binding.

The exciton peaks have also been observed at room temperature. The average temperature coefficients of the energy of the peaks between 4°K and room temperature is (in units of 10^{-4} eV/°C) -0.4 for the $Z_{1,2}$ peak, -0.3 for the Z_3 peak, -1.7 for the H_1, H_2, and H_3 peaks in CuI, -0.4 for the $Z_{1,2}$ peak in AgI, $+1.3$ for the $Z_{1,2}$ and Z_3 peaks in CuBr, and $+1.4$ for the same peaks in CuCl. The small value of these temperature coefficients compared with most zincblende semiconductors (~ -4) and its sign reversal from CuI to CuBr is somewhat surprising. This temperature coefficient stems from two different phenomena[27]: the thermal expansion of the lattice (volume effect) and the electron-phonon interaction (explicit temperature effect). The small value obtained for the total coefficient and its sign reversal suggests a compensation of the two effects. Since the sign of the coefficient due to the electron-phonon interaction is likely to be negative, a positive sign for the volume effect is to be expected, contrary to what happens for the [000] gap or other zincblende-like semiconductors.[28] The positive volume effect could be due to

[23] C. E. Moore, *Atomic Energy Levels*, National Bureau of Standards, Circular No. 467 (U. S. Government Printing Office, Washington, D. C., 1952), Vol. II.

[24] F. Herman, J. Electronics **1**, 103 (1955).

[25] C. E. Moore, *Atomic Energy Levels*, National Bureau of Standards, Circular No. 467 (U. S. Government Printing Office, Washington, D. C., 1958), Vol. III.

[26] The energy gap equals the energy of the first exciton peak plus the exciton ionization energy which is about 0.02 eV for these compounds.

[27] H. Brooks, *Advances in Electronics*, edited by L. Marton (Academic Press Inc., New York, 1957), Vol. 7.

[28] W. Paul, J. Phys. Chem. Solids **8**, 196 (1959).

a decreasing contribution of the metal wave function to the valence band wave function as the lattice constant is increased, which would produce an increase in the energy gap. The coefficient found for the H phase of CuI is much larger than that of the Z phase. This could be due to the increased electron-phonon interaction resulting from the larger number of atoms per unit cell which increases the number of optical-lattice-vibrations branches. Measurements of the pressure dependence of the exciton peaks will be performed in the future in order to determine directly the volume part of the temperature coefficient and test the interpretation given above.

B. Pseudobinary Alloys

The compounds discussed in the last section form three completely miscible pseudobinary systems: AgI–CuI, CuI–CuBr, and CuBr–CuCl. The exciton spectrum of the CuI–CuCl system, in the small miscibility range, is discussed in reference 15. Figure 5 shows the energy of the exciton peaks as a function of alloy concentration for the AgI–CuI system. The films were prepared by evaporating a known mixture of the components. The concentration was determined from the x-ray pattern by finding the lattice constant and using Vegard's law. Because of the closeness of the core potentials of Ag and Cu, we can describe the crystal potential at a metal site as the sum of a site-independent

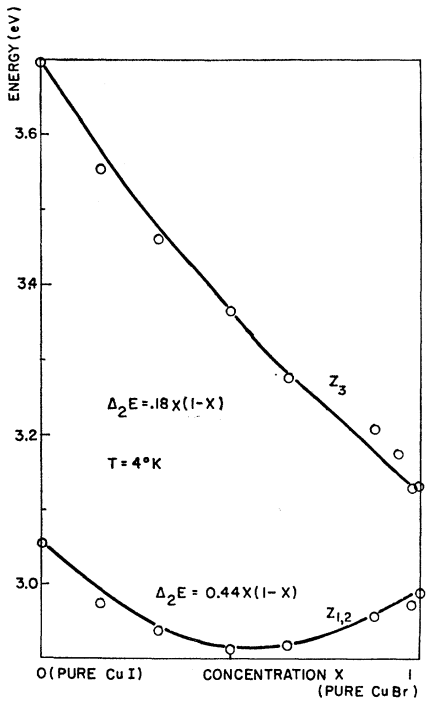

FIG. 6. Energy of the exciton peaks vs concentration in the CuI–CuBr system.

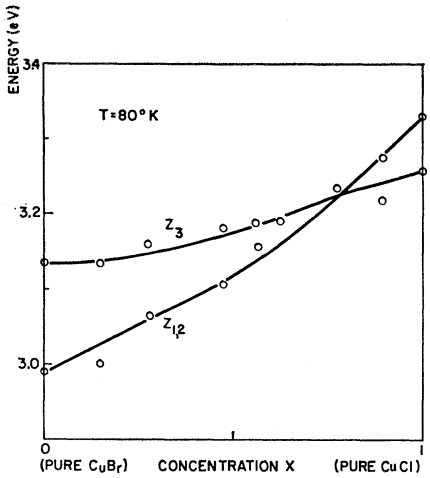

FIG. 7. Energy of the exciton peaks vs concentration in the CuBr–CuCl system.

average potential[29]:

$$V_1=xV_{Ag}+(1-x)V_{Cu} \tag{3}$$

plus a random perturbing potential V'. The potential V_1 produces a linear variation of the energy gap ($\sim$the position of the exciton peaks[26]) between the pure compounds. The potential V' produces a second-order perturbation Δ_2E proportional to the mean square deviation of the potential from the average potential V_1, hence,

$$\Delta_2E=Cx(1-x). \tag{4}$$

The difference between the linear and the experimentally found variation has been fitted in Fig. 5 using Eq. (4) and drawn as a full curve. The agreement between this curve for $C=0.58$ eV and the experimental points is good for the $Z_{1,2}$, W_1, and W_2 peaks. The agreement is

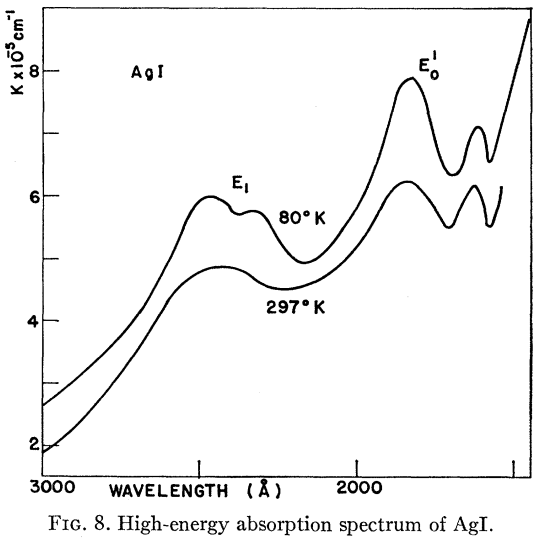

FIG. 8. High-energy absorption spectrum of AgI.

[29] R. Paramenter, Phys. Rev. **97**, 587 (1955).

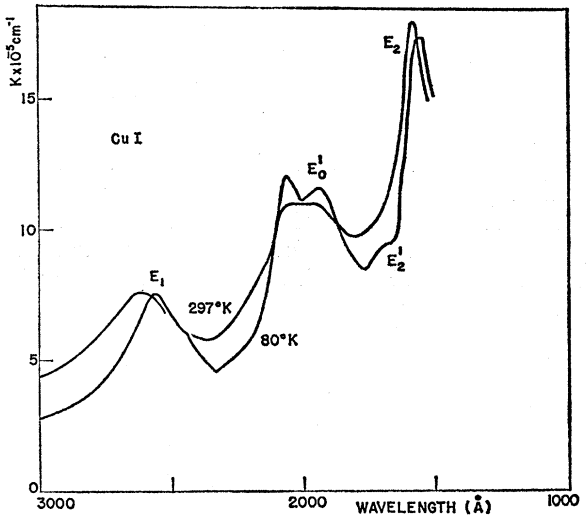

FIG. 9. High-energy absorption spectrum of CuI.

not as good for the Z_3 and W_3 peaks ($C\sim0.91$ eV) due probably to the changing proportion α of silver wave function in the valence band states. This change is not taken into account in Eq. (4). The good fit of the W_1 and W_2 peaks with Eq. (4) confirms the interpretation of these peaks in CuI as due to the presence of a small amount of wurtzite-type compound. A hexagonal phase was found in the samples by x rays for x up to 0.8.

Figure 6 shows the energy of the exciton peaks as a function of alloy concentration for the CuI–CuBr system. A good fit to the experimental points is obtained using Eq. (4) with $C=0.44$ eV for the $Z_{1,2}$ and $C=0.18$ for the Z_3 peak. The variation of Z_3 with x proves the nonlocalized nature of the excitons in these materials, since for localized excitons one should find in mixed

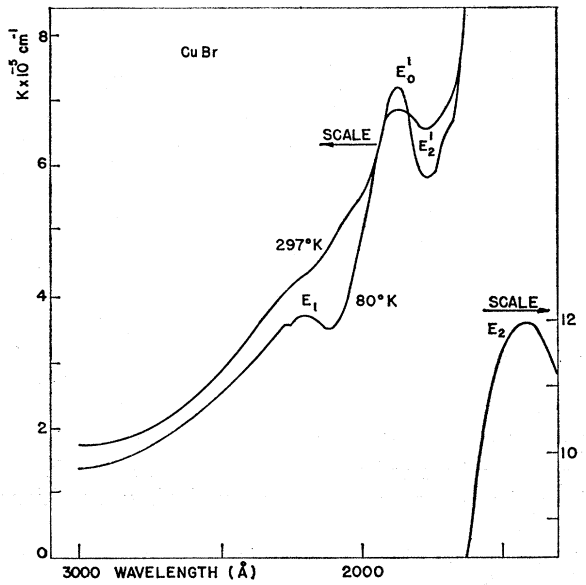

FIG. 10. High-energy absorption spectrum of CuBr.

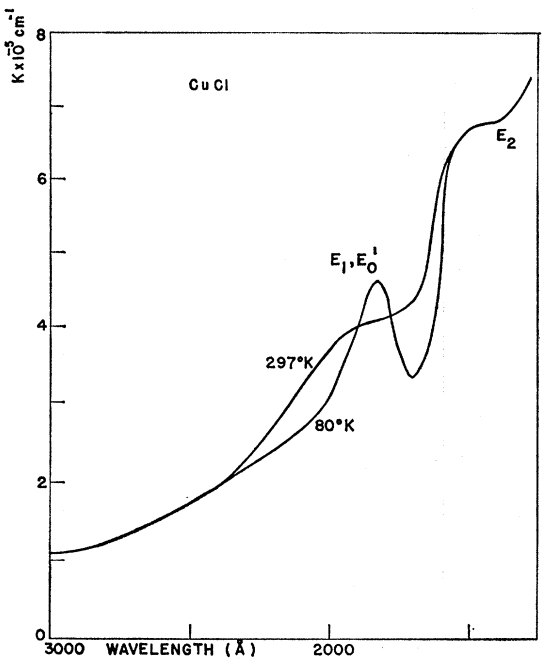

FIG. 11. High-energy absorption spectrum of CuCl.

crystals the peaks of the two components instead of just one peak at an energy between the two components, as discussed by Mahr for the KCl–KI system.[30]

The nonlocalized nature of the excitons is clearly apparent in Fig. 7 for the CuBr–CuCl system. The spin-orbit splitting goes to zero for $x=0.77$. The multiplet in CuCl is inverted in agreement with the conclusions of Sec. IV A.

The "anomalous" variation of the energy gap with concentration found for the zincblende-like systems ZnTe–ZnSe and InAs–GaAs[31] can also be explained with Eq. (4). The second-order perturbation seems to be much smaller in several other zincblende-like systems investigated (Si–Ge,[32,33] GaAs–GaP,[34] GaSb–AlSb[35]). The reason for the small value of C in these compounds may lie in the existence of short-range order which would decrease the random potential.

V. TRANSITIONS AT HIGHER ENERGIES

A. Absorption in the Pure Compounds

Figures 8, 9, 10, and 11 show the ultraviolet absorption spectrum of very thin evaporated films of AgI, CuI, CuBr, and CuCl at room and liquid-nitrogen temperature. Some of the structure present in these absorp-

[30] H. Mahr, Bull. Am. Phys. Soc. **6**, 114 (1961).
[31] S. Larrach, R. E. Schrader, and G. F. Stocker, Phys. Rev. **108**, 587 (1957); M. S. Abrahams, R. Braunstein, and F. D. Rosi, J. Phys. Chem. Solids **10**, 204 (1959).
[32] R. Braunstein, F. Herman, and A. Moore, Phys. Rev. **109**, 395 (1958).
[33] J. Tauc and A. Abraham, J. Phys. Chem. Solids **20**, 190 (1961).
[34] E. E. Loebner and W. Poor (private communication).
[35] I. I. Burdigan, Soviet Phys.–Solid State **1**, 1246 (1960).

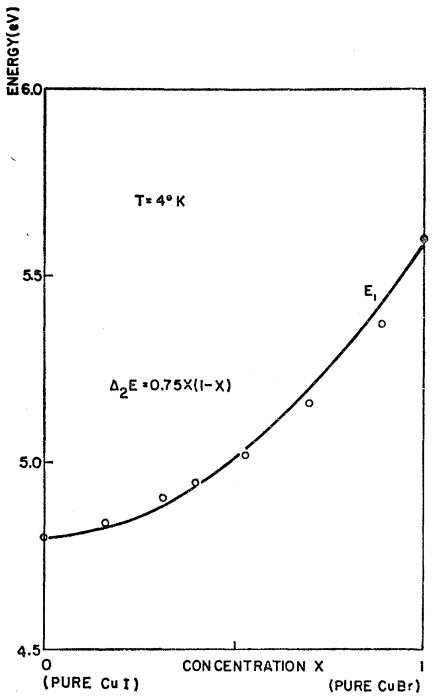

FIG. 12. E_1 peak in the CuI–CuBr system as a function of concentration.

tion spectra can also be seen in earlier work.[36] The salient features of these spectra become considerably clearer at lower temperatures. The spectra look similar to the spectra of Ge, Si,[37] and other zincblende-type semiconductors.[4] Thus it seems reasonable to interpret the present spectra along the same lines as the zincblende compounds. The stronger peak E_2 is believed to be due to the double singularity in the density of states for the transitions existing near the X point ([100]) direction, edge of the Brillouin zone). This maximum should split into two for materials without inversion symmetry (zincblende structure), since the X_1 point of the diamond structure splits into two (X_1-X_3) when the inversion symmetry is lifted. The shoulder E_2' seen at 1700 Å in the low-temperature absorption of CuBr, and CuI (Figs. 9 and 10) may be one of the components of the split peak, the other being at 1400 Å in CuBr and 1580 Å in CuI. This splitting arises in Herman's perturbation scheme[24] from a first-order perturbation splitting of the X_1 doublet by the antisymmetric potential and it should be proportional to the perturbation parameter λ. Therefore the splitting for CuBr (1.6 eV) should be about three times the splitting for GaAs in good agreement with recent measurements of this splitting (0.43 eV).[38] In CuCl (Fig. 11) the highest maximum in the absorption E_2 is beyond the range of our equipment. It has however been seen at 10 eV.[36] The split component of the E_2 peak (E_2) can be seen at 1500 Å; the splitting is 1.7 eV. This splitting could not be seen in AgI.

The peak next in intensity is labeled E_0'. In AgI it shows a splitting of 0.91 eV suggesting it may be due to transitions from the top of the valence band at $k=0$ (the splitting at this point found from the exciton spectrum is 0.84 eV). Hence, it seems reasonable to assign this peak to the same type of transitions which produce a similar peak in Si, GaP, and ZnSe: transitions between the Γ_{15} valence band maximum and the Γ_{15} conduction band minimum ($\Gamma_{25'}$ and Γ_{15} for the higher symmetry silicon structure). The splitting found for the E_0' peak in CuI from Fig. 9 (0.45 eV) is smaller than the exciton splitting (0.64 eV) but this may be due to the poor resolution of this peak or to the transitions occurring somewhat off $k=0$. The spin-orbit splitting is small compared with the peak broadening for the E_0' peak in CuBr and CuCl; it cannot be observed (see Figs. 10 and 11).

The lowest energy peak E_1 shows a low-temperature splitting of 0.4 ev in AgI, 0.29 in CuI, and 0.12 in CuBr. This peak is not seen in CuCl since, as we shall see in the next section, it lies under the stronger E_0' peak. Comparing these spectra with the spectra of other zincblende-like semiconductors it seems reasonable to attribute the E_1 peak to the transitions producing the low-energy peak in most of these semiconductors.[1] These transitions occur for k in the [111] direction. Until recently it was believed that the crystal momentum k for these transitions was at the edge of the Brillouin zone, but it has been suggested lately[39] that the peak is actually due to a saddle point in the energy difference between the valence and the conduction band occurring for k in the [111] direction somewhere inside the Brillouin zone. The spin-orbit splitting at such a point should also be about two-thirds of the splitting at $k=0$. The experimental splittings for CuI and AgI are somewhat smaller but a different contribution of the metal d wave functions to the valence band wave function could account for the small discrepancy.

Except for CuCl, in all these compounds the E_1 and E_0' peaks appear simultaneously as strong, well-defined peaks. In all other zincblende-like semiconductors measured, either the E_1 or the E_0' peaks could be observed clearly, the other peak appearing only very weakly because of its proximity to the stronger peak. The extraordinary sharpness with which these peaks are found in evaporated layers of silver and cuprous halides is also remarkable. In Ge and Si the conditions for the evaporation and the material of the substrate must be chosen very carefully in order to see any structure at all in the absorption.[40] For the III-V compounds these conditions

[36] E. G. Schneider and H. M. O'Bryan, Phys. Rev. **51**, 293 (1937); H. Fesefeldt, Z. Physik **67**, 37 (1931).
[37] H. R. Phillipp and E. A. Taft, Phys. Rev. **113**, 1002 (1959); **120**, 37 (1960).
[38] D. L. Greenaway, Phys. Rev. Letters **9**, 97 (1962).
[39] D. Brust, J. C. Phillips, and F. Bassani, Phys. Rev. Letters **9**, 94 (1962).
[40] M. Cardona and G. Harbeke (to be published).

are somewhat less critical and even less for the II-VI compounds. However, in none of these materials did the structure appear as clearly as in the silver and cuprous halides.

In Fig. 4 we have plotted the various energy peaks of the AgI isoelectronic sequence, without spin-orbit splitting perturbation,[2] as a function of the square of Herman's perturbation parameter λ. A linear dependence should be found for perturbations smaller than the energy separation between perturbing levels. This is not the case for the E_0' peak in AgI, since the $\Gamma_{25'}$ and the Γ_{15} levels of gray tin interact with each other through the antisymmetric perturbing potential. Figure 4 shows that the perturbation for AgI is larger than the separation between the $\Gamma_{25'}$ and the Γ_{15} level in gray tin. However, if we assume that only the interaction between these two levels is important in determining the AgI gap, we can write, by solving the 2×2 perturbation matrix:

$$(E_{\text{polar}}/E_{\text{nonpolar}})^2=1+2AE^{-1}{}_{\text{nonpolar}}\lambda^2. \qquad (5)$$

Equation (5) reduces to Eq. (1) for $2AE^{-1}{}_{\text{nonpolar}}\lambda^2\ll1$. This is likely to hold for the E_0 (fundamental gap), E_1, and E_2 gaps since the levels taking part in the transitions are not connected by an antisymmetric potential. The experimental points for these levels lie close to a straight line. For the E_0' peaks a reasonable fit is obtained with Eq. (5) as shown in Fig. 4. A similar fit for the cuprous halides is possible for the E_2 peaks but not for the other peaks, probably due to the large contribution of the $3d$ electrons of copper to the valence-band wave functions.

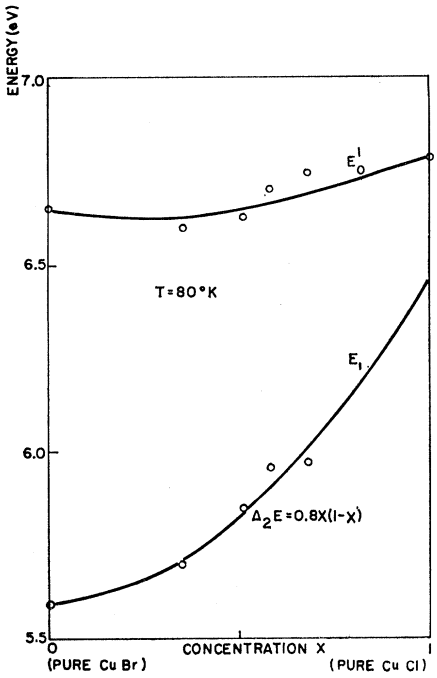

FIG. 13. E_1 and E_0' peaks in the CuBr–CuCl system as a function of concentration.

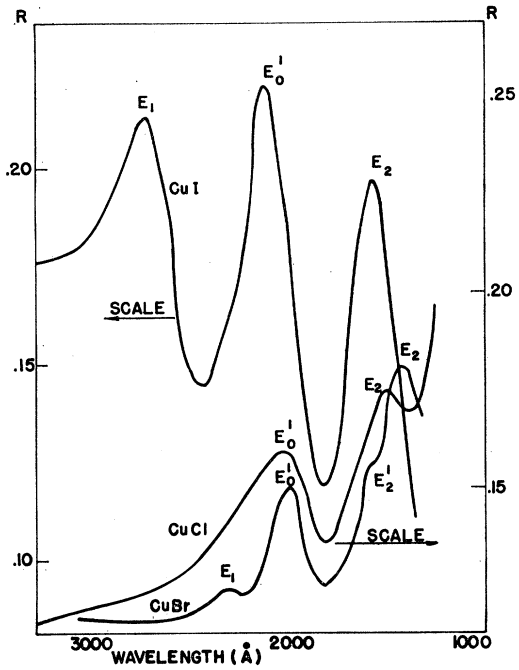

FIG. 14. Reflection spectrum of CuI, CuBr, and CuCl at room temperature.

B. Absorption in the Alloys

Figures 12 and 13 show the variation of the E_1 peak for the CuI-CuBr system and the E_1 and E_0' peaks for the CuBr–CuCl system, respectively, and the theoretical fit according to Eq. (4). Figure 13 shows why the E_1 peak is not seen in CuCl: It is very close to the stronger E_0' peak. The same thing probably occurs in in other compounds of the CuCl isoelectronic sequence (ZnS, GaP)[2]. By fitting the E_1 peaks in Fig. 13 to Eq. (4), one finds for the E_1 gap in CuCl 6.45 eV.

C. Reflection in the Pure Compounds

The structure described in the previous section was first observed in other zincblende-type semiconductors in the reflection spectrum of cleaved or etched single crystals. Figure 14 shows the reflectivity of CuI, CuBr, and CuCl evaporated layers measured at room temperature. The CuI sample was evaporated on a substrate at $T_s=400°$K and the CuBr and CuCl samples at room temperature. Higher T_s temperatures decreased the reflectivity and its structure. A strong analogy can be seen between the reflection and transmission spectra. The reflection peaks E_1 and E_0' occur at somewhat lower energies than the corresponding transmission peaks (see Table I). These reflectivity peaks are mainly

TABLE I. Peaks in the absorption and reflection spectrum of the zincblende-like silver and cuprous halides in eV.

	$Z_{1,2}$	Z_3	E_1		E_0'		E_2	
	Transmission 80°K		Transmission 80°K	Reflection 297°K	Transmission 80°K	Reflection 297°K	Transmission 80°K	Reflection 297°K
AgI	2.919	3.756	5.40 5.00	~5.4	6.80 7.71	6.9	8.7	···
CuI	3.059 3.047	3.692	5.10 4.81	4.6	6.40 5.98	6.0	7.9 7.3	8.0
CuBr	2.987	3.134	5.60 5.48	5.3	6.65	6.3	8.9 7.3	8.9 7.3
CuCl	3.306	3.237	6.45	···	6.79	6.1	10 8.3	··· 8.3

due to a maximum in the refractive index.[41] If the energy difference between the valence and the conduction band at the point where the transitions start is parabolic, the maximum in the refractive index should coincide with the beginning of the absorption edge. The maximum in the absorption will occur at the point at which the bands, deviating from its parabolic form, give a maximum in the combined density of states. Thus, in this case, the energy gap is given by the position of the reflection peak. However, if the transitions are due to an S_2-type saddle point[42] in the energy separation, the density of states $\eta(E)$ around this point will be:

$$\begin{aligned} &\eta(E)=B \quad \text{for} \quad E\geq E_1, \\ &\eta(E)=B-D(E_1-E)^{1/2} \quad \text{for} \quad E\leq E_1, \end{aligned} \tag{6}$$

where B and D are constants. In order to avoid negative values of η, we cut off η at the energy at which $\eta=0$ and make $\eta=0$ at any energy below that. The real part of the polarizability will be proportional to the integral

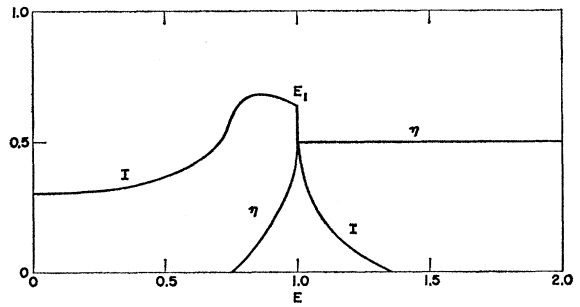

FIG. 15. Density of states and polarizability around an S_2-type saddle point.

(Kramers-Kronig relations):

$$I=\int_0^\infty \frac{\eta(E')}{(E'^2-E^2)E'}dE'. \tag{7}$$

Figure 15 shows the integral I for the density of states:

$$\begin{aligned} &\eta(E)=0 \quad &&\text{for} \quad E\leqslant 0.75, \\ &\eta(E)=(0.25)^{1/2}-(1-E)^{1/2} \quad &&\text{for} \quad 0.75\leqslant E\leqslant 1, \\ &\eta(E)=(0.25)^{1/2} \quad &&\text{for} \quad E\geqslant 1. \end{aligned}$$

Figure 15 shows that Eq. (7), and hence the reflectivity, has a maximum at an energy lower than the singularity $E_1=1$. The absorption spectrum will show a sharp change of slope (peak) at the energy E_1 of the singularity. Hence, we see that, depending on the type of singularity involved, either the energy of the absorption peak or that of the reflection peak gives the energy E_1 of the singularity. We cannot conclusively decide which type of singularity produces the E_1 structure. The E_0' peak seems to be due, in several other semiconductors with the same structure,[39] to a minimum at $k=0$. This is probably also the case in the materials under consideration and therefore the energy at which the E_0' reflection peak occurs gives the Γ_{15}–Γ_{15} energy gap.

The reflectivity of several evaporated AgI layers was also measured. The structure was not as pronounced as in the cuprous halides but several peaks corresponding to the peaks in the transmission spectrum were observed. Their energies are listed in Table I.

ACKNOWLEDGMENTS

I wish to thank Oleh Tkal for preparing the samples and performing some of the measurements, R. Paff and W. Roth for the x-ray measurements and D. S. McClure, R. Paramenter, and R. E. Shrader for several discussions.

[41] M. Cardona and H. S. Sommers, Jr., Phys. Rev. **122**, 1382 (1961).
[42] L. Van Hove, Phys. Rev. **89**, 1189 (1953).